Investigations of the dynamics of road pavement reflectance

Kang Jiang (姜 亢)[1,2], Kai Yu (于 凯)[1], and Yongchao Zhao (赵永超)[1*]

[1]*Key Laboratory of Technology in Geo-Spatial Information Processing and Application System, Institute of Electronics, Chinese Academy of Sciences, Beijing 100190, China*

[2]*Graduate University of Chinese Academy of Sciences, Beijing 100049, China*

[*]*Corresponding author: ofcours_sure@sina.com*

Received August 1, 2011; accepted November 7, 2011; posted online January 6, 2012

Road pavement reflectance is usually assumed to be invariant in short periods of time in some quantitative remote sensing applications. To examine its variability, reflectance sequences of concrete and asphalt pavement are measured in field for half a day in visible and near-infarecd (VNIR) spectral range using dual-beam method. As much as 20.7% and 3.52% of relative changes are found in asphalt and concrete reflectance data at 550 nm, and all VNIR bands demonstrate similar variations found to correlate with both illumination geometry and the relative portion of diffuse irradiance. In this letter, this effect is interpreted from a mathematic view. Further studies are needed to model the dynamics of reflectance physically.

OCIS codes: 240.0240, 240.5698, 280.0280.

doi: 10.3788/COL201210.042401.

Reflectance of road pavement is usually believed to be invariant in a short period of time due to the physical and chemical stabilities of the pavement. Therefore, road surfaces are often selected as pseudo-invariant feature (PIF) targets in relative radiometric normalization among images[1,2] and vicarious calibrations of remote sensors[3,4]. Although studies on the reflective features of road pavement are very limited, existing results indicate that pavement reflectance varies according to various factors. Herold *et al.*[5,6] found that the amplitude of overall reflectance and certain absorption bands varies with age. Puttonen *et al.*[4,7] measured the bi-directional reflectance distribution factor (BRDF) of asphalt and concrete pavements separately, demonstrating that pavement reflectance varies according to viewing geometry. Anderson *et al.*[3] measured 30-min time sequences of the reflectance of asphalt and concrete pavements, identifying measurable changes in the reflectance data. These results demonstrate that assuming the reflectance of road pavement to be invariant in a short time period will bring systematic uncertainty to applications like vicarious calibration.

Despite the previously mentioned existing studies, knowledge about reflective features of road pavements is still incomplete. Most published studies on road pavement reflectance focus on its BRDF under fixed or only several discrete sun angles; the reflectance response to the change of illumination condition has not been fully discussed. Given that many studies indicate that the reciprocity of BRDF for a structured surface is invalid[8], the continuous measurement of reflectance under changing illumination conditions is then necessary to get a full understanding of its reflectance behavior to conduct modeling studies on surface reflectance[9]. In Ref. [3], time sequence measurements only lasted 30 min, during which time the dynamic range of sun angles and illumination amplitude is relatively small, meaning the data cannot present full reflectance response to the illumination condition.

We measured the reflectance sequences of two concrete road samples and three asphalt pavement samples in the visible and near-infared (VNIR) spectral range for half the daytime hours using the dual-beam method. Since the dynamics of the illumination condition are nearly symmetrical within the entire day, half of the daytime hours are sufficient to cover the range of sun illumination. Reflectance data were collected every 10 s using fixed viewing geometry, thereby obtaining a continuous reflectance response of these samples based on the change of illumination.

A dual-beam method was adopted in the measurement. Compared with the single-beam method[10], the dual-beam method can minimize possible inaccuracies that might result from changing atmospheric conditions and field of view[11]. Two kinds of dual-beam methods can be used: based on the cosine receptor and based on the reference panel. The difference between the two lies in the way of obtaining total irradiance E: the cosine receptor method records E directly while the reference panel method calculates E using reflected radiance from the reference panel.

Samples from a concrete parking lot and asphalt road pavement, which were usually selected as PIF, were used for the measurements. The selected parking lot was located in an open area with no tall buildings or trees around within 500 m, so scattered illumination from surroundings could be minimized. Figure 1(a) shows the concrete surface. Meanwhile, asphalt pavement samples were collected from a road construction site and measured on top of a 17-floor building to avoid scattered illumination from surroundings. The new asphalt, shown in Fig. 1(b), had been produced several days before the measurement; the old asphalt samples 1 and 2, shown in Figs. 1(c) and (d), were taken from heavy and minor traffic areas, respectively.

ASD FieldSpec FR (400–2 500 nm) and FieldSpec HH (325–1 075 nm) spectrometers were used in the dual-beam measurements. A FieldSpec remote cosine receptor (RCR) and a 50% reference panel were used to obtain global irradiance in two different methods. A 99% refer-

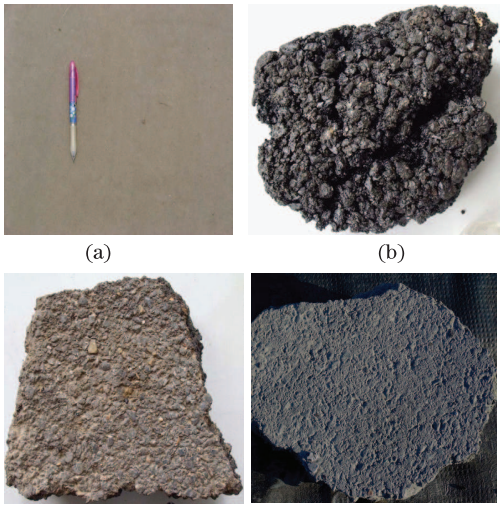

(a) (b) (c) (d)

Fig. 1. Road pavement samples used in the measurements of (a) concrete parking lot, (b) new asphalt pavement, and old asphalt samples (c) 1 and (d) 2.

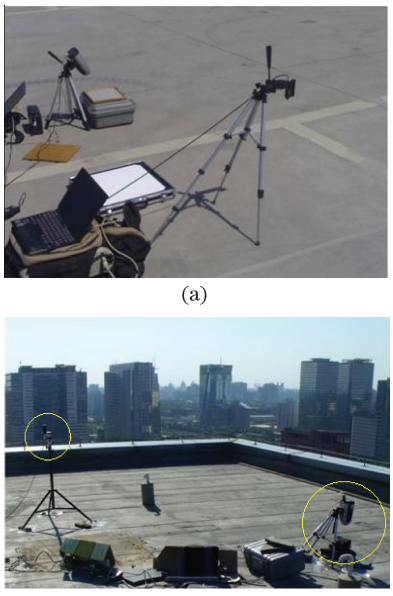

(a) (b)

Fig. 2. Device configuration in measurements of (a) concrete pavement (conducted *in situ*) (b) asphalt pavement samples (conducted on the roof of a tall building to avoid shadows or scatter light from surrounding buildings).

ence panel was used for inter-calibration between spectrometers. The device configuration is shown in Fig. 2. In concrete measurements, the probe of FieldSpec FR was adjusted to view vertically downwards using bubbles; FieldSpec HH was tilted about 25° southwards to prevent shadowing on the reference panel during measurements. In asphalt measurements, the RCR was adjusted vertically upward using bubbles while FieldSpec HH was tilted about 10° southwards to prevent shadowing on samples. Both spectrometers collected one spectrum every 10 s. RCR was shaded every 15 min to collect skylight diffuse irradiance. Five reflectance sequences of two concrete samples, one new asphalt sample, and two old asphalt samples were obtained. The basic information of these measurements are summarized in Table 1.

The reflectance measured in the field was a hemisphere-directional reflectance factor (HDRF), formulated as

$$R^{\mathrm{HDRF}}(t) = \frac{\pi L(\theta_{\mathrm{v}}, \varphi_{\mathrm{v}}, t)}{E(t)}, \tag{1}$$

where θ_{v}, φ_{v}, and t are view zenith, view azimuth angles, and time, respectively; $L(\theta_{\mathrm{v}}, \varphi_{\mathrm{v}}, t)$ is the target radiance recorded by the spectrometer from the direction $(\theta_{\mathrm{v}}, \varphi_{\mathrm{v}})$ at time t; $E(t)$ is the total irradiance at the bottom of atmosphere at time t. $E(t)$ was recorded by the other spectrometer through RCR or reference panel.

Many non-target factors in the measurement may influence $R^{\mathrm{HDRF}}(t)$, and they are removed before the reflectance calculation using the following preprocessing steps:

(i) Synchronize $L(\theta_{\mathrm{v}}, \varphi_{\mathrm{v}}, t_1)$ and $E(t_2)$ with local time t_0. Differences between t_0 and two controls for computer times t_1, t_2, denoted as Δt_1 and Δt_2, are recorded before measurement and are used to revise time stamps of sequences, i.e. $L(\theta_{\mathrm{v}}, \varphi_{\mathrm{v}}, t_1 + \Delta t_1)$, $E(t_2 + \Delta t_2)$.

(ii) Estimate and remove the floating of dark current (DC) of the two spectrometers, denoted as $\Delta\mathrm{DC}(t)$. DC is manually collected before and after the measurement to determine the change of DC. $\Delta\mathrm{DC}(t)$ is then estimated using linear interpolation over the entire measurement period and is distracted from the raw DN sequences.

(iii) Inter-calibrate two spectrometers. Probes of the two spectrometers are collocated, pointing vertically downward, and simultaneously collect reflected radiance from the 99% reference panel. The panel is positioned with several slope angles or shaded to create several lightness levels. Calibration coefficients can then be calculated using linear regression of these data.

After the preprocessing steps, reflectance sequences can then be calculated: if RCR is used for $E(t)$, reflectance is calculated according to Eq. (1); if a reference panel is used for $E(t)$, the reflectance is calculated using the following equation:

Table 1. Basic Information of Four Reflectance Sequence Measurements

Target	Date	Time	Sun Elev.	Spec. No.	Device
Con. 1	09/05/31	07:45–12:20	32.2–71.9	2679	*A*: 50% Ref *B*: Con.1
Con. 2	09/06/01	11:30–15:30	71.7–45.7	2108	*A*: 50% Ref *B*: Con.2
As. New	11/05/13	06:00–11:10	11.2–63.5	1721	*A*: As.new *B*: RCR
As. Old 1	11/05/13	11:10–18:45	65.4–3.1	2497	*A*: As.old 1 *B*: RCR
As. Old 2	11/10/01	07:00–12:00	8.46–46.1	2601	*A*: As.old 2 *B*: 50%Ref

A: FieldSpec HH spectrometer *B*: FieldSpec FR spectrometer.

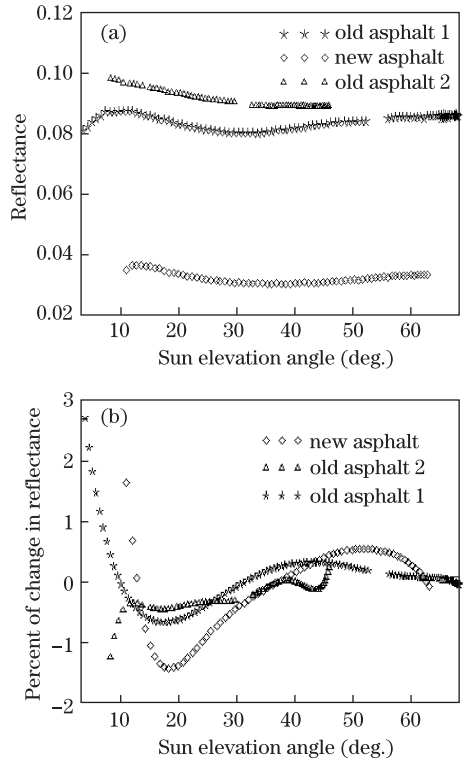

Fig. 3. (a) Notable variation in reflectance of all asphalt samples in 550 nm; (b) $\Delta\mathrm{ref}[\theta_\mathrm{i}(k)]$ of all samples in 550 nm.

$$R^{\mathrm{HDRF}}(t) = \frac{L(\theta_\mathrm{v}, \varphi_\mathrm{v}, t)}{L^R(\theta_\mathrm{v}^R, \varphi_\mathrm{v}^R, t)} \cdot R \cdot c(\theta_\mathrm{v}^R), \tag{2}$$

where $L^R(\theta_\mathrm{v}^R, \varphi_\mathrm{v}^R, t)$ is radiance of reference panel recorded from direction $(\theta_\mathrm{v}^R, \varphi_\mathrm{v}^R)$ at time t; R is the hemisphere-directional reflectance of the reference panel measured from zenith in lab; $c(\theta_\mathrm{v}^R)$ is the directional reflectance factor of the reference panel in θ_v^R. R and $c(\theta_\mathrm{v}^R)$ are provided in the calibration files.

Notable variations were found in the reflectance sequences of concrete and asphalt pavement. During the measurement, illumination changed in three aspects: amplitude, sun angles, and ratio of diffuse-to-global irradiance (D/G). Amplitude and other multiplicative parameters are ratioed out[9], so reflectance response is only discussed on the other two aspects.

Reflectance variation of new and old asphalt samples with a sun elevation angle θ_i at 550-nm wavelength is presented in Fig. 3(a). The shapes of the three sequence curves are alike, indicating that new and old asphalt pavements have similar reflectance responses to the change of θ_i. The maximum variation of reflectance sequence relative to its mean value is denoted as

$$\Delta\mathrm{ref} = \frac{\mathrm{Max}\{R^{\mathrm{HDRF}}(\theta_\mathrm{i})\} - \mathrm{Min}\{R^{\mathrm{HDRF}}(\theta_\mathrm{i})\}}{\mathrm{Mean}\{R^{\mathrm{HDRF}}(\theta_\mathrm{i})\}}. \tag{3}$$

Δref of new, old sample 1, and old sample 2 reach 20.7%, 9.05%, and 10.6%, respectively. This variation is sufficiently large and may produce major inaccuracies in applications that assume asphalt reflectance as invariant. The percent of change in reflectance for a 1° change of θ_i is denoted as

$$\Delta\mathrm{ref}[\theta_\mathrm{i}(k)] = \frac{R^{\mathrm{HDRF}}[\theta_\mathrm{i}(k+1)] - R^{\mathrm{HDRF}}[\theta_\mathrm{i}(k)]}{R^{\mathrm{HDRF}}[\theta_\mathrm{i}(k+1)] + R^{\mathrm{HDRF}}[\theta_\mathrm{i}(k)]} \cdot \frac{200}{\theta_\mathrm{i}(k+1) - \theta_\mathrm{i}(k)}, \tag{4}$$

where k is the sequence index. $\Delta\mathrm{ref}[\theta_\mathrm{i}(k)]$ of all samples are presented in Fig. 3(b). For a 1° change of θ_i, all samples changed rapidly when $\theta_\mathrm{i} < 30°$. $\Delta\mathrm{ref}[\theta_\mathrm{i}(\mathrm{k})]$ of old asphalts are closer to zero than new asphalt in most θ_i ranges, indicating that the reflectance of old asphalt is more stable than that of new asphalt. Variations in other typical bands are summarized in Table 2.

The variation reflectance of two concrete pavement samples with θ_i at 550 nm is presented in Fig. 4(a). Discontinuity in the sequences is caused by a power problem during the measurements. In the $40° < \theta_\mathrm{i} < 70°$ range, Δref of concrete samples 1 and 2 reach 2.77% and 3.52%, respectively. $\Delta\mathrm{ref}[\theta_\mathrm{i}(k)]$ of two concrete samples are presented in Fig. 4(b). Both samples present similar rates of change, which increase as θ_i exceeds 60°.

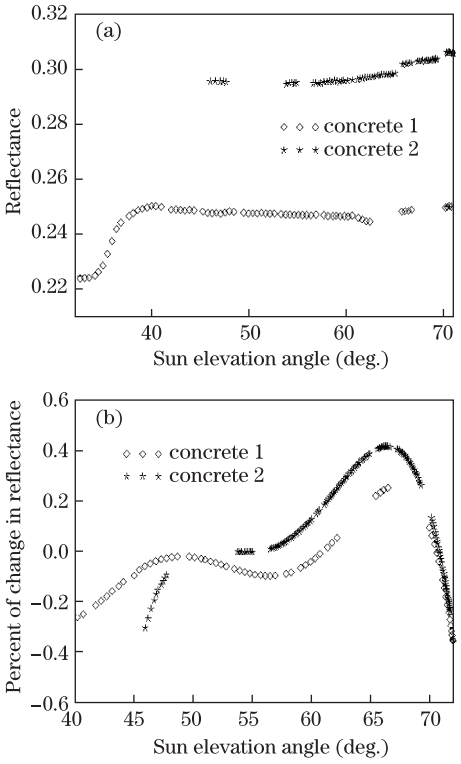

Fig. 4. (a) Reflectance variation of two concrete samples at 550 nm; (b) $\Delta\mathrm{ref}[\theta_\mathrm{i}(k)]$ of both samples at 550 nm in $40° < \theta_\mathrm{i} < 72°$.

Table 2. Relative Changes of Reflectance in Percent. Statistics Range from 10° to 65° Sun Elevation for Asphalt and 40° to 70° for Concrete

	483 nm	565 nm	660 nm	825 nm
Old Asphalt 1	7.55	11.4	9.54	13.4
Old Asphalt 2	10.5	10.1	12.3	12.6
New Asphalt	11.5	26.2	30.4	49.1
Concrete 1	2.45	2.76	2.91	4.93
Concrete 2	3.66	3.38	3.39	3.68

In the $30^\circ < \theta_\mathrm{i} < 40^\circ$ range, reflectance of concrete 1 has a sharp increase as its Δref reaches 11.5%, which is primarily caused by the reflectance variation of the reference panel (see Fig. 5). As the dashed box in Fig. 5 indicates, the radiance of concrete increases steadily as θ_i increases while the radiance sequence of the panel is fluctuant (see Fig. 5(b)). The data were collected early in the morning with a clear sky. The illumination amplitude increased steadily in this range, which is a reasonable inference from radiance sequence of concrete in Fig. 5(a). The fluctuating shape of the panel radiance sequence indicates that the reflectance of the reference panel changes according to illumination geometry.

The reflectance dynamics described above can be interpreted from a mathematical view. The recorded radiance at time t can be viewed as an integral of directional irradiance from all directions in the hemisphere:

$$L(\theta_\mathrm{v},\varphi_\mathrm{v},t)=\int_0^{2\pi}\int_0^{\pi/2}R(\theta_\mathrm{i},\varphi_\mathrm{i},\theta_\mathrm{v},\varphi_\mathrm{v}) \cdot L(\theta_\mathrm{i},\varphi_\mathrm{i},t)\cos\theta_\mathrm{i}\mathrm{d}\theta_\mathrm{i}\mathrm{d}\varphi_\mathrm{i}, \quad (5)$$

where $R(\theta_\mathrm{i},\varphi_\mathrm{i},\theta_\mathrm{v},\varphi_\mathrm{v})$ is the BRDF of the target; $L(\theta_\mathrm{i},\varphi_\mathrm{i},t)$ is the incident radiance from direction $(\theta_\mathrm{i},\varphi_\mathrm{i})$. Its distribution reflects the illumination geometry and amplitude. According to Eq. (1), the measured HDRF can then be written as

$$R^{\mathrm{HDRF}}(t)=\pi\int_0^{2\pi}\int_0^{\pi/2}R(\theta_\mathrm{i},\varphi_\mathrm{i},\theta_\mathrm{v},\varphi_\mathrm{v}) \cdot L^0(\theta_\mathrm{i},\varphi_\mathrm{i},t)\cos\theta_\mathrm{i}\mathrm{d}\theta_\mathrm{i}\mathrm{d}\varphi_\mathrm{i}, \quad (6)$$

where $L^0(\theta_\mathrm{i},\varphi_\mathrm{i},t)=L(\theta_\mathrm{i},\varphi_\mathrm{i},t)/E(t)$ can be viewed as normalized directional incident radiance. For an anisotropic $R(\theta_\mathrm{i},\varphi_\mathrm{i},\theta_\mathrm{v},\varphi_\mathrm{v})$, it is easy to see from Eq. (6) that $R^{\mathrm{HDRF}}(t)$ may change only if the distribution of $L^0(\theta_\mathrm{i},\varphi_\mathrm{i},t)$ over the hemisphere is changed. This effect is exhibited as temporal dynamics of reflectance in field measurements. Our measurements demonstrate that the reflectance of asphalt, concrete pavement, and reference panel all vary based on illumination geometry.

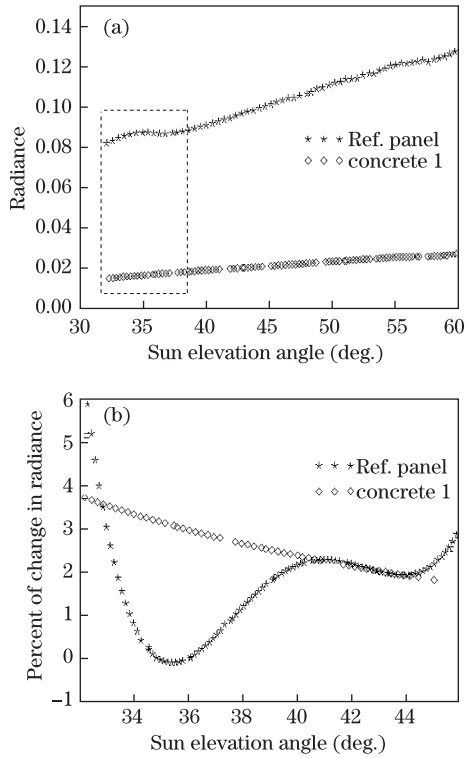

Fig. 5. (a) Sequences of radiance reflected by concrete sample 1 and the 50% reference panel; (b) $\Delta\mathrm{rad}[\theta_\mathrm{i}(k)]$ of concrete and panel at 550 nm in $30^\circ < \theta_\mathrm{i} < 45^\circ$.

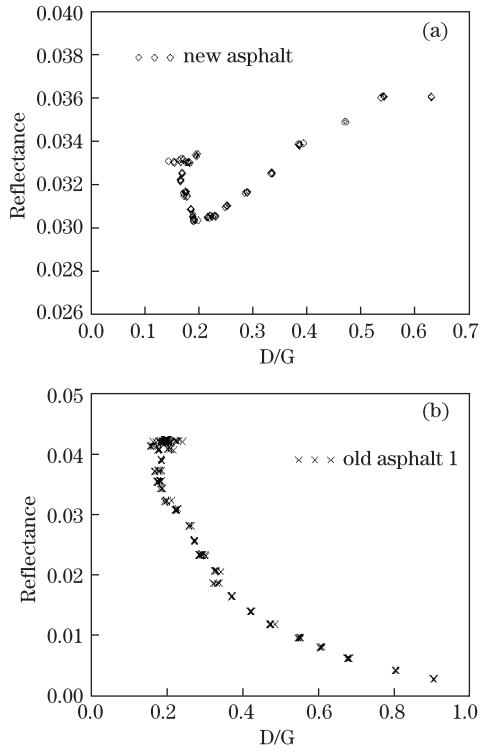

Fig. 6. Variations in reflectance of (a) new asphalt and (b) old asphalt sample 1.

Δref of asphalt and concrete samples in multiple bands are summarized in Table 2. The center wavelength of Landsat TM VNIR bands are used for statistics. It can be seen that Δref is generally larger in longer wavelengths than in shorter wavelengths and Δref of asphalt samples is generally larger than concrete samples. These results indicate that reflectance dynamics exist throughout the VNIR spectral region.

The scatterplots of asphalt reflectance against D/G values are presented in Fig. 6. Reflectance and D/G values show a high correlation for both asphalt samples when D/G is greater than 0.2, whereas their changing tendencies are opposite: new asphalt reflectance increases as D/G increases; old asphalt reflectance reacts contrarily. These results correspond with previously published results[3], where old asphalt reflectance also decreases as D/G increases, but the correlation between the reflectance and D/G is low ($r^2 = 0.53$). When D/G is lower than 0.2 (e.g., when it approaches noon), the reflectance and D/G are not correlated, indicating that D/G influences targets reflectance more under lower sun elevations.

Interesting phenomena are observed from these measurements. The results demonstrate that the reflectance of road pavement in the VNIR region is unstable and can fluctuate during half of the daytime period. The reflectance of the reference panel also changed in our mea-

surements; thus, we suggest that a cosine receptor should be used to obtain the total irradiance instead of reference panel in outdoor reflectance sequence measurements. It is highly possible that a change in the illumination condition, rather than physical or chemical variations of these targets, is the main cause of their reflectance dynamics. This effect is explained from a mathematical view. It may be reasonable to presume that the reflectance of all structured rough surfaces changes based on the illumination condition[12,13]. Reflectance models of many other land covers, such as forest, soil, and snow, support this presumption. Further studies on the reflectance model of road pavement are needed to interpret these phenomena physically and model its reflectance behavior quantitatively.

In conclusion, we investigate the dynamics of road pavement reflectance, detecting notable reflectance variations of both concrete and asphalt samples in our measurement. Applications that use road pavement as PIF target should take this effect into consideration.

This work was supported by the National 863 Program of China under Grant No. 2009AA122002. The authors wish to acknowledge Professor Su-hong Liu at Beijing Normal University and Professor Wen-jie Fan at Beijing University for providing the spectrometers.

References

1. D. L. Helder, B. Basnet, and D. L. Morstadb, Can. J. Rem. Sens. **36,** 527 (2011).
2. B. Clark, J. Suomalainen, and P. Pellikka, ISPRS J. Photogram. Rem. Sens. **66,** 429 (2011).
3. K. Anderson, E. J. Milton, and E. M. Rollin, in *Proceedings of IEEE International Geoscience and Remote Sensing Symposium* 2072 (2003).
4. E. Puttonen, J. Suomalainen, T. Hakala, and J. Peltoniemi, IEEE Trans. Geosci. Rem. Sens. **47,** 2330 (2009).
5. M. Herold, D. A. Roberts, M. E. Gardner, and P. E. Dennison, Rem. Sens. Environ. **91,** 304 (2004).
6. M. Herold and D. Roberts, Appl. Opt. **44,** 4327 (2005).
7. G. Meister, "Bidirectional reflectance of urban surfaces" PhD. Thesis (Hamburg University, 2000).
8. S. Liang, *Quantitative Remote Sensing of Land Surfaces* (J. Wiley & Sons, New Jersey, 2004).
9. H. Wu and L. Tong, Chin. Opt. Lett. **9,** 102901 (2011).
10. B. Curtiss and A. F. H. Goetz, in *Proceedings of International Symposium on Spectral Sensing Research* (1994).
11. S. J. Bolsenga and R. D. Kistler, J. Appl. Meteor. **21,** 642 (1982).
12. I. Renhorn and G. Boreman, Opt. Express **16,** 12892 (2008).
13. V. Y. Mendeleyev and S. N. Skovorodk, Opt. Express **19,** 6822 (2011).